

Designing a Gel-Fiber Composite to Extract Nanoparticles from Solution

Ya Liu, Xin Yong,[†] Gerald McFarlin, IV, Olga Kuksenok, Joanna Aizenberg,[§] Anna C. Balazs*

Chemical Engineering Department, University of Pittsburgh, Pittsburgh, PA 15261

[†]Department of Mechanical Engineering, Binghamton University, State University of New York, Binghamton, NY, 13902-6000

[§]Wyss Institute for Biologically Inspired Engineering, Department of Chemistry and Chemical Biology, and School of Engineering and Applied Science, Harvard, Cambridge, MA, 02138

Supporting Information

We demonstrate that the shrinking of the thermo-responsive gel exerts a negligible effect on the dynamics of relatively stiff fibers. Here, we focus on stiff fibers characterized by $K_{angle}^f = 10^3$; these are the most flexible of the fibers considered in our simulations, and thus, the conclusions obtained for this case will be particularly applicable for the stiffer fibers considered in our study. The initial configuration of the system is shown in Fig. S1a; this is the same setup as in Fig. 2a, except that the particle has been removed from the simulation box. To maintain the total bead number density at $\rho_{sys} = 3$ in the absence of the particle, we utilize 91,227 solvent beads in the simulation. The system is instantaneously heated to $T = 48^\circ\text{C}$.

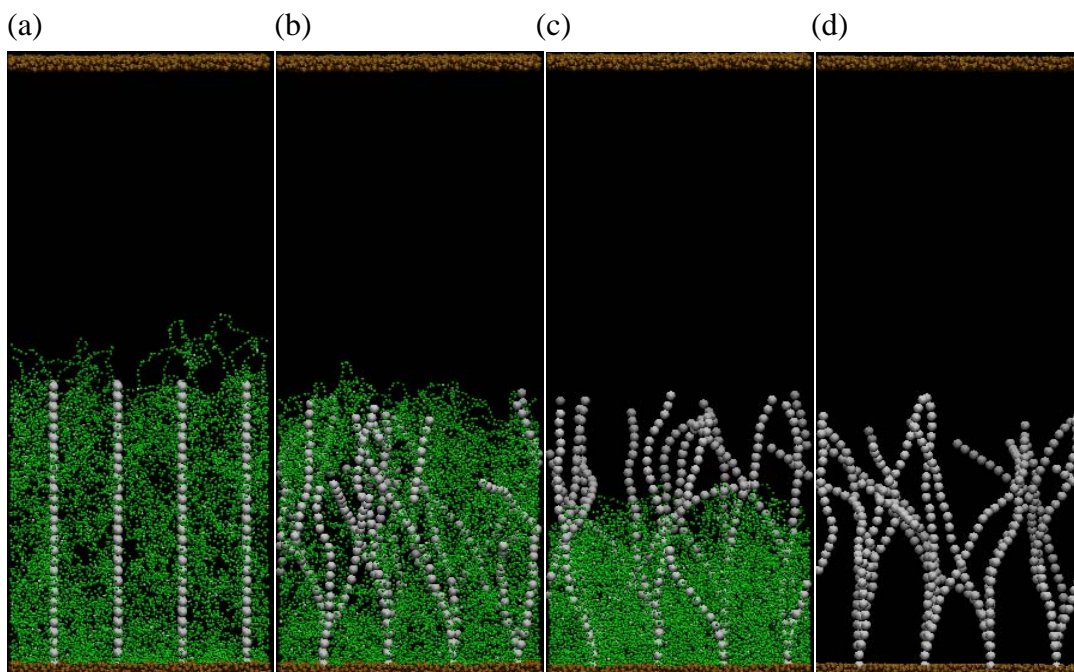


Figure S1. a)-c) Snapshots of the system for $a_{gf} = 25$ at $t = 0$, 4×10^5 , and 2×10^6 , respectively.

d) Snapshot of the fibers immersed in the solvent in the absence of the gel at $t = 2 \times 10^6$.

The gel can influence the dynamic behavior of the fibers through the following two ways: 1) an unfavorable enthalpic interaction, characterized by a_{gf} , and 2) the excluded-volume repulsion due to the topological connectivity of the polymer network. To isolate the effect of the excluded volume interactions, we set all the relevant repulsion parameters to $a_{ij} = 25$ (see Table S1). Namely, by setting the interaction parameters between the fibers and solvent (a_{sf}) and between the fibers and gel (a_{gf}) to the same value, we can eliminate the effect of the enthalpic contributions on the behavior of the fibers. We did not, however, change the gel-solvent interaction parameter, which characterizes the thermo-responsive behavior of the polymer network. Recall that the gel exhibits an LCST, and thus, collapses as the temperature is increased, as shown in Figs. S1b-c. At $T=48^\circ\text{C}$ and $t=4\times10^5$, the effectively hydrophobic gel is seen to shrink towards the bottom wall (Fig. S1b); at this early time, the height of the gel lies close to the height of the extended fibers. The deformation of these fibers is due to thermal fluctuations.

	Solvent	Fiber	Top Wall	Bottom Wall	Polymer Gel
Solvent	25	25	25	25	χ_{ps}
Fiber	-	25	25	25	a_{gf}
Top Wall	-	-	25	25	25
Bottom Wall	-	-	-	25	a_{gw}
Polymer Gel	-	-	-	-	25

Table S1: List of interaction parameters in units of reduced temperature, T^* .

As the gel keeps shrinking, the fibers become more exposed to the surrounding solvent; these fibers do not self-assemble into bundles (see Fig. S1c at $t = 2\times10^6$) because the fiber-solvent and fiber-fiber interaction are equivalent. Figure S1d shows an image at from a separate simulation that involves just the end-tethered fibers immersed in the solvent; here $t = 2\times10^6$. By comparing Figs. S1c and S1d, we see that the fibers are unaffected by the shrinking gel.

We can quantify the dynamic behavior of the system by monitoring the temporal evolution of the center of mass of the fibers, as shown in Figure S2. Each solid curve represents an average over four independent simulations and the shading about the curves represents the corresponding standard deviations. The black curve is the center of mass of the fiber in the system depicted in Figure S1d (i.e., in the absence of the gel). The latter curve rapidly reaches an equilibrium value, as shown in Fig. S2 (displaying relatively large fluctuations). The red curve in the plot shows the behavior of the fibers in the presence of the neutral gel ($a_{gf} = 25$). At early times (for $t < 2\times10^5$), this red curve approaches an equilibrium value more slowly than the black curve; thereafter, however, the discrepancy between the black and red curves disappears. Since the curves for the fibers in the absence and presence of the neutral gels eventually show the same

behavior, the results indicate that the gel-fiber excluded-volume interactions during the collapse of this gel do not affect the late-stage behavior of these fibers.

The green curve in Fig. S2 shows the temporal evolution for the center of mass of the fiber for the case where the gel-fiber interaction is more repulsive and is characterized by $a_{gf} = 40$; this is the scenario considered in the main text (see Table 1). Notably, the three curves overlap when $t > 1 \times 10^6$, suggesting that the shrinking of the relatively incompatible gel exerts a negligible effect on the dynamics of the stiff fibers considered in our study. (Due to the stronger enthalpic repulsion for $a_{gf} = 40$, the fibers exhibit less deformation at the early stages than in Fig. S1b.)

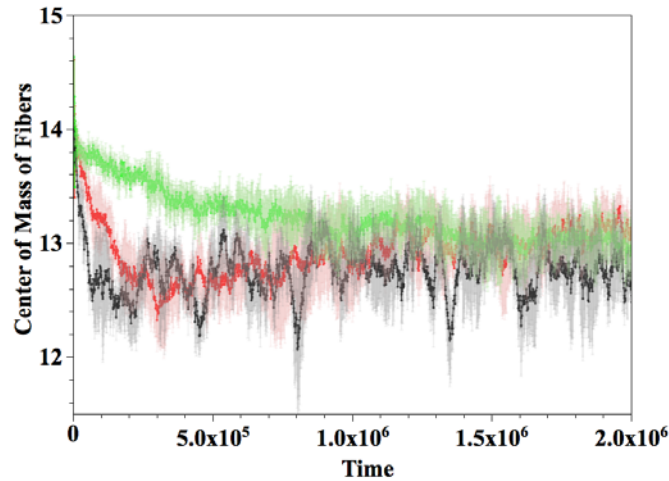


Figure S2. Temporal evolution of the center of mass of the fibers for the cases when the gel-fiber interaction parameter $a_{gf} = 25$ (red) and 40 (green), and for the pure fiber system (black).